Drug Development and Industrial Pharmacy, 26(6), 621–633 (2000)

RESEARCH PAPER

Evaluation and Validation of a Fully Instrumented Hüttlin HKC 05-TJ Laboratory-Scale Fluidized Bed Granulator

K. Wöstheinrich and P. C. Schmidt

University of Tübingen, Department of Pharmaceutical Technology, Auf der Morgenstelle 8, D-72076 Tübingen, Germany

ABSTRACT

The instrumentation and validation of a laboratory-scale fluidized bed apparatus is described. For continuous control of the process, the apparatus is instrumented with sensors for temperature, relative humidity (RH), and air velocity. Conditions of inlet air, fluidizing air, product, and exhaust air were determined. The temperature sensors were calibrated at temperatures of 0.0°C and 99.9°C. The calibration of the humidity sensors covered the range from 12% RH to 98% RH using saturated electrolyte solutions. The calibration of the anemometer took place in a wind tunnel at defined air velocities. The calibrations led to satisfying results concerning sensitivity and precision. To evaluate the reproducibility of the process, 15 granules were prepared under identical conditions. The influence of the type of pump used for delivering the granulating liquid was investigated. Particle size distribution, bulk density, and tapped density were determined. Granules were tableted on a rotary press at four different compression force levels, followed by determination of tablet properties such as weight, crushing strength, and disintegration time. The apparatus was found to produce granules with good reproducibility concerning the granule and tablet properties.

INTRODUCTION

Fluidized bed technology for pharmaceutical purposes offers considerable advantages over the multistage process of conventional wet granulation (1,2). To produce granules with reproducible technical and biopharmaceutical properties, reliable monitoring of the granulation process is required.

The instrumentation of a fluidized bed granulator is described by several authors (3,4). Variables that influence product properties can be distinguished as apparatus variables, process variables, and product variables. The influence of apparatus variables such as position of the nozzle and atomizing air pressure and their effects on granule growth kinetics were described (4–7). Other authors investigated process variables like spray rate, airflow rate, and temperature (3,6,8,9). Product variables such as the quantity and distribution of the binder were also analyzed (9,10). To control the process and to determine the end point, an approach using near-infrared spectroscopy was performed (11). A theoretical approach considering material and thermal energy balances during fluidized bed granulation was made by Scott et al. (12). Further investigations in the field of pharmaceutical fluidized bed granulation were published by Kristensen and Schæfer (13) and Banks and Aulton (14).

In this paper, the evaluation of the laboratory-scale fluidized bed granulator Hüttlin Kugelcoater HKC 05-TJ is described. The apparatus is equipped with sensors for temperature, airflow rate, and humidity in order to describe exactly the conditions during the process. The temperature sensors were calibrated at temperatures of 0.0°C and 99.9°C. Calibration of the humidity sensors was performed at a range of 12% relative humidity (RH) to 98% RH using saturated electrolyte solutions. The anemometer was calibrated using a wind tunnel with air speeds varying from 5 m/sec to 20 m/sec. The response times of the sensors were evaluated. To prove the reproducibility of the process, 15 batches of lactose monohydrate were granulated using an aqueous solution of lactose monohydrate and polyvinylpyrrolidone (PVP) without any variations of process or product parameters. The influence of the pump type supplying the granulator with the binder solution was determined using a peristaltic pump or two piston pumps calibrated in advance. The granule properties were determined. Tablets were prepared at four different compression forces using an instrumented rotary tablet press. Tablet properties such as crushing strength and disintegration time were analyzed.

MATERIALS AND METHODS

Materials

Lactose monohydrate (GranuLac 200, Meggle, Wasserburg, Germany) and PVP (Kollidon 90 F, BASF AG, Ludwigshafen, Germany) were used for the preparation of the granules. Tablets were compressed after the addition of 4% cross-linked PVP (Kollidon CL, BASF AG) as the disintegrant and 1% magnesium stearate (Bärlocher, Munich, Germany) as the lubricant.

Equipment

The following instruments were used: Hüttlin Kugelcoater HKC 05-TJ with two 3-component nozzles (BWI Hüttlin, Steinen, Germany); Pt-100 temperature sensors (no. 6041.7114); fan-wheel anemometer (no. 0635.9345) and combined relative humidity/NTC temperature sensors (no. 0636.2260); data logger Testo 454 and software Comfort Light, version 2.1 (Testo, Lenzkirch, Germany); Excel 97 as software for further exploitation (Microsoft Corp., Unterschleissheim, Germany); control unit for the heater Jumo dTron (Juchheim, Fulda, Germany); peristaltic pump (505S/RL, Watson-Marlow, Falmouth, UK) and two piston pumps (LCP 4000, Biotek GmbH, Östringen, Germany); laser diffraction spectrometer Sympatec HELOS KA Compact with a RODOS distribution unit (Sympatec, Clausthal-Zellerfeld, Germany); tapped density tester JET ST2 (Engelmann AG, Ludwigshafen, Germany); mixer Turbula T2C (Willy Bachofen, Basel, Switzerland); rotary tablet press PH 103 (Korsch Pressen GmbH, Berlin, Germany); electronic balance AE 200 (Mettler-Toledo, Gieβen, Germany); tablet hardness tester Schleuninger 6D (Schleuninger, Solothurn, Switzerland); and tablet disintegration tester PTZ 1 (Pharmatest, Hainburg, Germany).

Description of the Apparatus

Figure 1 shows a schematic diagram of the Kugelcoater with the installed sensors. Air enters into the apparatus through a metal pipe to which a Pt-100 temperature sensor and a fan-wheel anemometer are attached; an exact specification of the inlet airflow is thus provided. The inlet air is filtered; air temperature and relative humidity are measured by a sensor (capacitive reactance humidity/NTC temperature sensor) located behind the inlet air filter. Air passes an electric heater, and constant temperatures of the fluidizing air are provided by the heater con-

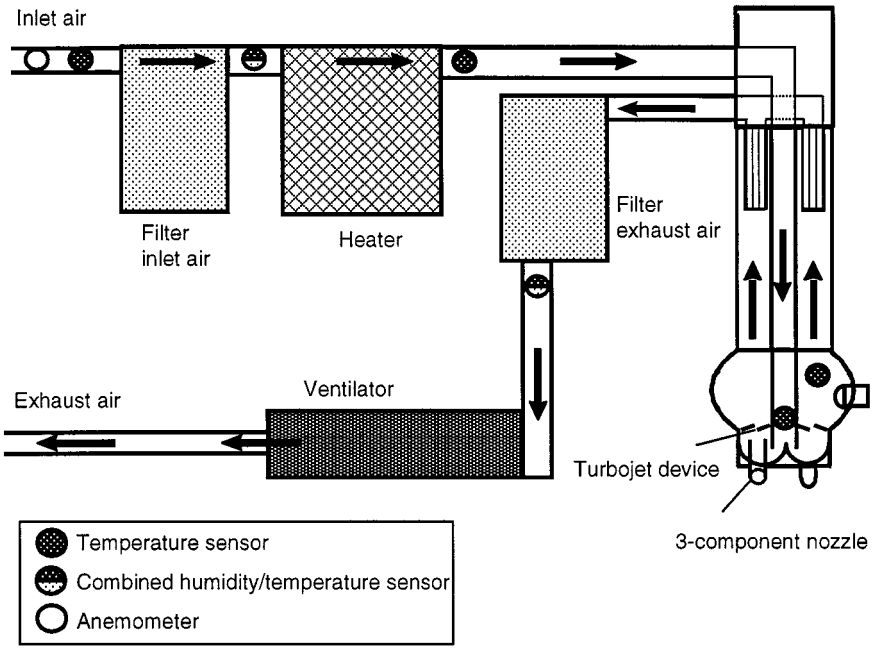

Figure 1. Scheme of the Hüttlin Kugelcoater HKC 05-TJ with its instrumentation.

trol unit working with Pt-100 sensors. Before finally entering the product chamber, the warm air passes through a pipe with a Pt-100 sensor located at the very end of it. This temperature is considered the exact temperature at which the fluidizing air enters into the powder bed. The fluidizing device, the Turbojet, consists of eight single blades, forming a rotor that accelerates the fluidizing air (Fig. 2). After passing the temperature sensor, the warm air is reversed, passes through the gaps between the blades of the Turbojet device, and fluidizes the powder.

Granulating liquid is sprayed tangentially into the powder bed by two 3-component nozzles located face to face within the Turbojet device. The nozzles consist of a central pipe that provides granulation liquid surrounded by a second pipe that delivers atomizing air. A third tube encircling the inner parts supplies the nozzle with the microclimate. This leads to lower temperatures and increased relative humidities within a cone-shaped area in front of the atomizing nozzle compared to the conditions in the powder bed. Droplets forming in front of the nozzle are transported by the microclimate in the direction of the powder bed, thus keeping the tip of the nozzle clear.

The powder performs a tangential movement, and granulating liquid is bottom-sprayed in the same direction. The temperature of the fluidized bed is measured 8 cm above the Turbojet device by a Pt-100 sensor. The humid exhaust air leaves the product chamber through five dynamic filters. Obstructions of the filters are avoided by compressed air blown through the fabric filter bags alternately 90 times per minute.

Humidity and temperature of the exhaust air are measured by a combined sensor located behind the outlet air filter. Constant airflow is provided by an electric ventilator at the bottom of the unit. The ventilator is controlled by a potentiometer.

Data from the sensors are first distributed to a data logger and then transmitted to a personal computer (IBM 86-386) for on-line output with the software installed. Further exploitations are performed using MS Excel 97.

Calibration

Temperature sensors were dipped into ice-water mixtures at 0.0°C and boiling water at 99.9°C. For each temperature, 10 determinations were performed after an equilibration time of 3 min.

Humidity sensors were calibrated at room temperature (20°C) using saturated electrolyte solutions with relative humidities ranging from 12% RH to 98% RH. Sensors were put into sealed glass vessels containing the saturated electrolyte solution; the sensor was located 5 cm above the liquid. After 10 min equilibration time, the data were taken; for each level of humidity, five measurements per sensor were performed.

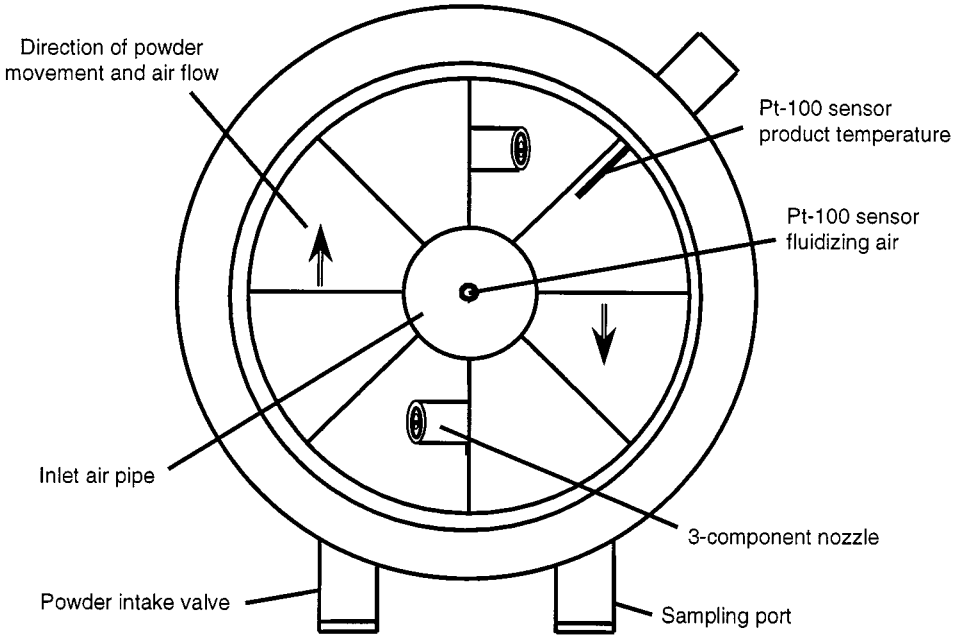

Figure 2. Scheme of the Turbojet device.

The anemometer was calibrated by the manufacturer using a wind tunnel with laser Doppler anemometer. Measurement took place in the center of a low-turbulent free open jet with a diameter of 350 mm with defined airflow ranging from 5.0 m/sec to 20.0 m/sec.

For the calibration of each sensor slope, intercept and correlation coefficient were calculated (Table 1).

To evaluate response times, the temperature sensors were first kept at room temperature (20°C) and then inserted into an airflow of 65°C with a speed of 10 m/sec. These conditions simulate very well the terms of the process. Three determinations were made for each sensor. For an evaluation of the response times of the humidity sensors, the sensors were inserted into the glass ves-

Table 1

Calibration Data of the Sensors

Sensor	Calibration Method	Calibration Function	Correlation Coefficient
Fan-wheel anemometer	Laser-Doppler device in wind tunnel, 5.0–20.0 m/sec	$y = 0.9920x + 0.050$	1.0000
Pt-100 temperature sensor (inlet air)	Water at 0°C and 99.7°C	$y = 0.9878x + 0.010$	1.0000
Capacitive reactance humidity sensor (inlet air)	Saturated electrolyte solutions, 12–98% RH	$y = 0.9919x + 0.7604$	0.9998
NTC temperature sensor (inlet air)	Water at 0°C and 99.7°C	$y = 0.9233x + 1.5508$	0.9964
Pt-100 temperature sensor (fluidizing air)	Water at 0°C and 99.7°C	$y = 0.9897x - 0.060$	1.0000
Pt-100 temperature sensor (product temperature)	Water at 0°C and 99.7°C	$y = 0.9907x + 0.9906$	1.0000
Capacitive reactance humidity sensor (outlet air)	Saturated electrolyte solutions, 12–98% RH	$y = 0.9813x + 1.4219$	0.9999
NTC temperature sensor (outlet air)	Water at 0°C and 99.7°C	$y = 0.9274x + 1.3037$	0.9974

Table 2

Response Times of the Sensors in Air During Alterations of Temperature or Relative Humidity

Temperature Sensors	Mean Response Time During Heating from 20°C to 65°C (sec)	Mean Response Time During Cooling from 65°C to 20°C (sec)
Pt-100 sensor inlet air	46	39
Pt-100 sensor fluidizing air	44	38
Pt-100 sensor product	46	37
NTC temperature sensor inlet air	122	68
NTC temperature sensor outlet air	116	74
Humidity Sensors	**Mean Response Time During Decrease from 85% RH to 40% RH (sec)**	**Mean Response Time During Increase from 85% RH to 40% RH (sec)**
Capacitive reactance sensor inlet air	33	31
Capacitive reactance sensor outlet air	31	30

sels used for the calibration, which provided conditions of 85% RH at room temperature. After equilibration, the time needed for adaptation to room conditions of 39% RH was determined. On the other hand, sensors adapted to room conditions were inserted into the glass vessel with 85% RH. The results given in Table 2 are the mean of three determinations. All response times are the times needed for adaptation to 95% of the final value.

Both the peristaltic pump and the piston pumps were calibrated by pumping granulating liquid. As the kinematic viscosity of the granulating liquid strongly depends on the temperature, the temperature was kept constant at 20°C, 25°C, or 30°C during the calibration of the pumps. The output of liquid over 2 min was determined using an electronic balance at three different pump speeds. Five determinations for each temperature and pump speed were performed. As a result, each temperature level was regarded separately, and three calibration functions with their correlation coefficients were obtained for each pump (Table 3).

Granulation and Tableting

To estimate reproducibility of the granulating process, 15 batches were produced. For 7 batches, the peristaltic pump was used; the other 8 batches were prepared by delivering the granulating liquid with two piston pumps. Using a solution of 10% lactose monohydrate and 5%

Table 3

Calibration of the Pumps Used for Granulation

Pump Calibrated	Temperature of the Granulating Liquid During Calibration (°C)	Calibration Function	Correlation Coefficient
Peristaltic	20	$y = 3.6905x + 1.4055$	0.9976
	25	$y = 3.6942x + 0.9448$	0.9982
	30	$y = 3.7093x + 0.8317$	0.9978
Upper piston	20	$y = 1.2495x + 0.0607$	0.9997
	25	$y = 1.3695x - 0.1973$	0.9998
	30	$y = 1.3530x - 0.0707$	0.9995
Lower piston	20	$y = 1.9903x + 0.0927$	0.9998
	25	$y = 2.0238x + 0.0960$	0.9999
	30	$y = 2.0320x + 0.0780$	0.9999

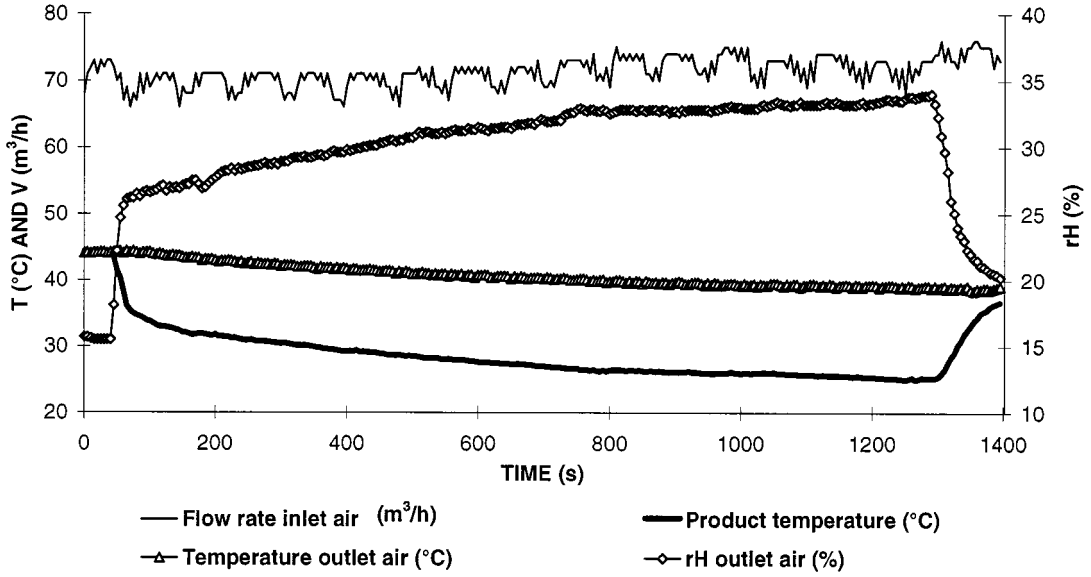

Figure 3. Typical course of outlet air humidity, airflow rate and product, and outlet air temperature during a granulation process.

PVP in purified water, 400 g of lactose monohydrate were granulated. The spray rate was kept constant at 10 g/min; the amount of granulating liquid was 200 g; and temperature the of the fluidizing air was 50°C. Atomizing pressure was kept constant at $3 \cdot 10^4$ Pa; the pressure used for the microclimate was 10^4 Pa. During the whole process, data of the sensors were distributed every 10 sec to the data logger and the personal computer. Typical courses for inlet airflow, outlet air humidity and product, and outlet air temperature during a process are shown in Fig. 3.

The granules prepared using the peristaltic pump were

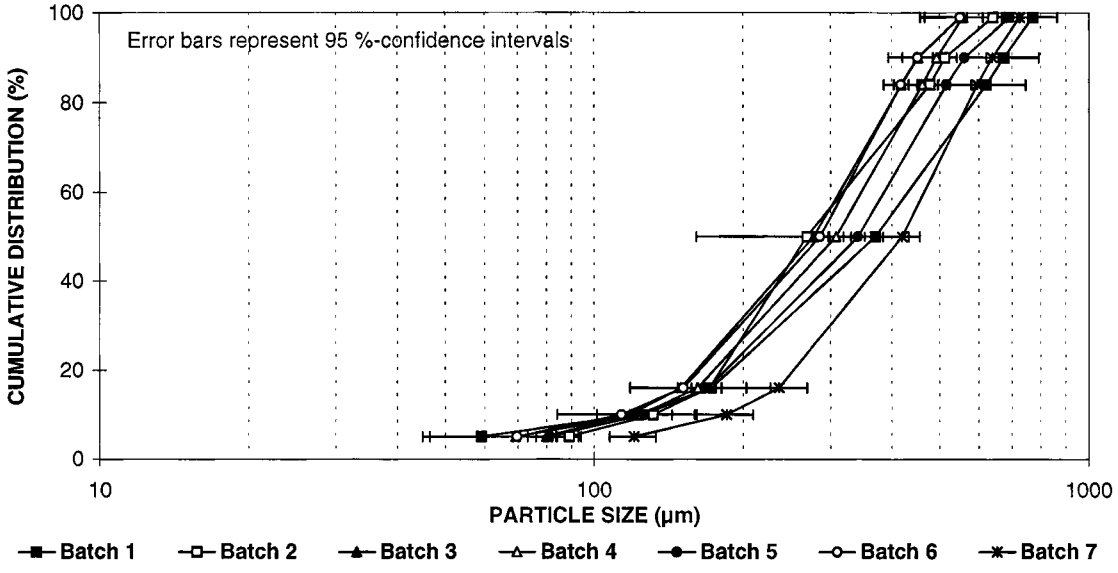

Figure 4. Particle size distributions of seven formulations granulated using the peristaltic pump ($N = 2$).

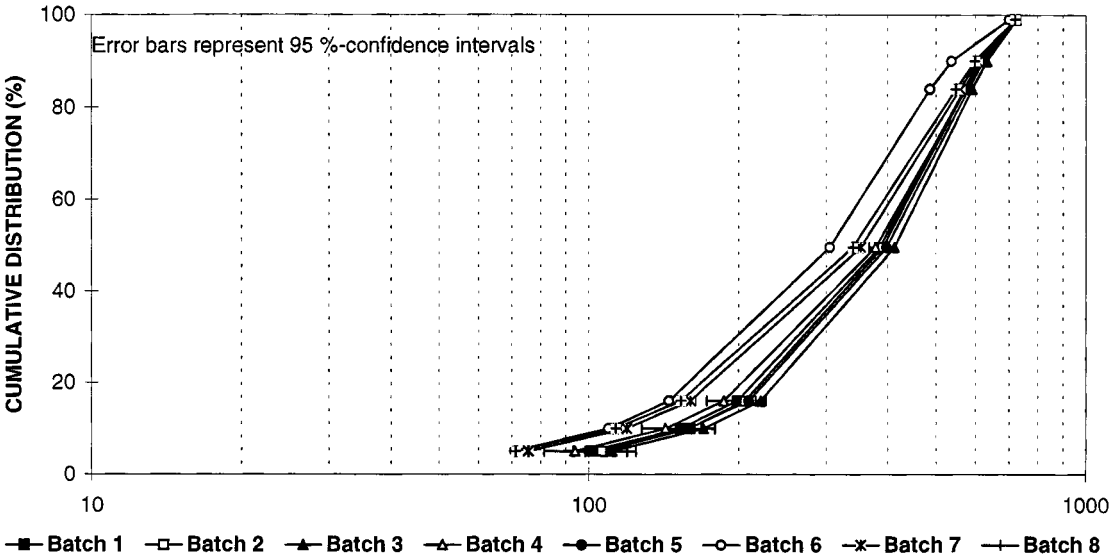

Figure 5. Particle size distributions of eight formulations granulated using the piston pumps ($N = 2$).

Table 4

Bulk Density, Tapped Density, and Hausner Value of Lactose Granulation Batches

Granulation	Batch	Bulk Density (g/ml)	Tapped Density (g/ml)	Hausner Value
Prepared with peristaltic pump	1	0.423	0.472	0.896
	2	0.390	0.472	0.826
	3	0.379	0.454	0.834
	4	0.396	0.471	0.841
	5	0.384	0.463	0.829
	6	0.362	0.439	0.825
	7	0.391	0.463	0.844
Mean		0.389 ± 0.019	0.462 ± 0.012	0.842 ± 0.025
Standard deviation		4.76%	2.62%	2.95%
Prepared with piston pumps	1	0.368	0.413	0.891
	2	0.368	0.420	0.875
	3	0.382	0.427	0.894
	4	0.380	0.407	0.935
	5	0.394	0.443	0.890
	6	0.345	0.400	0.862
	7	0.364	0.420	0.869
	8	0.364	0.420	0.869
Mean		0.371 ± 0.016	0.419 ± 0.014	0.886 ± 0.025
Standard deviation		4.28%	3.29%	2.82%

Table 5

Properties of Tablets Made from Lactose Preparations Granulated with the Peristaltic Pump

Batch No.	C (kN)	CS (N)	W (mg)	D (min)
1	5.84 ± 0.25	—	293.80 ± 3.62	16.0
	11.62 ± 0.55	3.9 ± 1.0	291.63 ± 2.55	15.0
	15.29 ± 1.21	5.8 ± 0.6	294.02 ± 3.70	13.0
	20.93 ± 1.61	9.1 ± 1.0	291.34 ± 4.62	12.0
2	6.29 ± 0.49	—	316.24 ± 4.79	17.0
	11.36 ± 0.73	4.5 ± 0.7	321.67 ± 3.84	16.0
	16.61 ± 0.94	7.0 ± 1.1	322.83 ± 3.31	14.0
	20.45 ± 1.43	10.4 ± 1.4	325.06 ± 3.25	12.0
3	5.73 ± 0.17	—	318.72 ± 3.68	14.0
	9.76 ± 0.47	3.8 ± 0.4	323.01 ± 3.59	16.25
	15.86 ± 0.89	7.3 ± 0.7	324.42 ± 3.56	14.25
	21.52 ± 1.26	10.7 ± 1.1	327.29 ± 3.25	13.0
4	5.62 ± 0.24	—	309.10 ± 7.70	14.0
	9.84 ± 0.93	3.5 ± 0.5	319.53 ± 5.09	16.0
	15.64 ± 1.47	6.9 ± 0.9	322.26 ± 4.43	15.5
	20.47 ± 1.76	9.2 ± 1.2	318.10 ± 5.21	14.0
5	6.03 ± 0.26	—	322.00 ± 5.80	17.0
	9.48 ± 0.60	4.2 ± 1.1	324.88 ± 4.09	18.0
	14.67 ± 1.06	7.4 ± 1.0	326.23 ± 4.42	16.0
	21.75 ± 1.57	11.6 ± 2.0	325.55 ± 4.32	13.0
6	5.86 ± 0.38	—	316.74 ± 5.47	17.5
	9.53 ± 0.69	3.7 ± 0.7	324.80 ± 5.50	16.5
	15.14 ± 0.91	7.7 ± 1.1	327.00 ± 3.77	15.0
	21.34 ± 1.28	11.1 ± 1.2	326.82 ± 4.40	14.0
7	6.40 ± 0.55	—	293.75 ± 4.08	18.0
	9.77 ± 1.07	3.6 ± 0.7	301.40 ± 6.49	14.0
	16.70 ± 2.01	5.9 ± 1.0	305.51 ± 6.85	14.0
	18.69 ± 1.86	8.0 ± 1.3	307.94 ± 6.06	12.5

C = compression force; CS = crushing strength; W = weight; D = disintegration time.

sieved to separate single agglomerates with particle sizes exceeding 800 μm. This withdrawn portion was not more than 2% of the whole batch. As no agglomerates occurred when delivering the granulating liquid with the piston pumps, no sieving had to be performed for those granules.

Granule size distributions were determined using a laser diffraction spectrometer with the RODOS distributing unit. Figure 4 shows the cumulative distribution of seven lactose-PVP granulations prepared using the peristaltic pump. Cumulative particle size distributions of the granules derived using the piston pumps are shown in Fig. 5.

For the determination of the bulk density, 50 g of the granules were filled into a graduated 250-ml measuring cylinder; the occupied volume was determined. The same cylinder was then inserted into a JET ST2 tapping device and tapped 1250 times. For each granule, two determinations of the bulk and tapped densities were made (Table 4). The Hausner ratio, defined as the ratio of tapped density to poured density, was calculated.

Granular materials, 4% cross-linked PVP, and 1% magnesium stearate were mixed for 10 min using a Turbula T2C mixer at 42 rpm. Tablets were compressed using 10-mm beveled-edge tooling with an instrumented rotary tablet press. The compression forces ranged from 5 to 20 kN in intervals of 5 kN. During a period of 20 sec, all compression forces were recorded, and mean value and standard deviation were calculated. To monitor tablet uniformity, the masses of 10 tablets per level were determined using an electronic balance. The crushing strength of 10 tablets was analyzed using a Schleuninger Tablet Hardness Tester 6D. Disintegration times of 6 tablets each were determined in purified water at 37°C using a Pharmatest PTZ 1 apparatus. All results are given in Tables 5 and 6.

Table 6

Properties of Tablets Made from Lactose Preparations Granulated with the Piston Pumps

Batch No.	C (kN)	CS (N)	W (mg)	D (min)
1	6.72 ± 0.23	—	316.56 ± 4.61	16.0
	9.77 ± 0.41	3.5 ± 0.5	319.65 ± 3.28	14.5
	14.02 ± 0.85	5.4 ± 0.5	314.96 ± 3.56	14.0
	18.03 ± 1.03	8.3 ± 0.7	294.29 ± 3.50	12.0
2	5.90 ± 0.19	—	310.08 ± 5.03	14.5
	9.00 ± 0.73	—	297.48 ± 3.82	13.0
	14.91 ± 0.47	5.5 ± 0.5	315.40 ± 1.96	12.5
	22.25 ± 0.84	9.0 ± 0.8	312.97 ± 3.02	12.5
3	6.56 ± 0.28	—	310.87 ± 4.49	17.0
	10.91 ± 0.49	3.6 ± 0.5	312.87 ± 3.60	15.5
	16.85 ± 0.73	6.1 ± 0.9	315.07 ± 4.05	13.0
	22.44 ± 1.25	9.7 ± 1.2	317.52 ± 3.48	13.0
4	6.20 ± 0.16	—	309.63 ± 1.93	14.0
	11.91 ± 0.45	4.1 ± 0.3	314.85 ± 3.80	12.0
	15.64 ± 0.71	6.1 ± 0.3	317.28 ± 2.55	12.0
	19.39 ± 0.63	8.0 ± 1.3	316.84 ± 1.77	10.5
5	6.53 ± 0.29	—	318.88 ± 2.37	14.5
	10.85 ± 0.33	3.5 ± 0.5	327.97 ± 2.16	13.0
	16.20 ± 0.63	6.1 ± 0.3	331.42 ± 1.65	13.0
	20.57 ± 1.00	8.6 ± 0.7	330.00 ± 4.12	11.5
6	6.08 ± 0.10	—	304.50 ± 2.85	17.0
	9.65 ± 0.44	3.6 ± 0.7	310.59 ± 2.33	16.0
	16.20 ± 0.59	5.7 ± 0.5	312.28 ± 2.85	14.5
	22.57 ± 0.95	10.1 ± 0.9	311.83 ± 2.69	13.0
7	6.27 ± 0.28	—	319.25 ± 3.55	16.5
	11.02 ± 0.46	4.1 ± 0.3	325.89 ± 1.56	14.5
	15.00 ± 0.39	6.2 ± 0.4	327.63 ± 2.46	13.5
	20.00 ± 0.67	8.6 ± 0.5	325.18 ± 3.63	13.0
8	6.22 ± 0.20	—	319.91 ± 3.47	15.5
	9.85 ± 0.34	3.5 ± 0.7	323.47 ± 2.82	15.0
	15.25 ± 0.43	6.0 ± 0.0	325.81 ± 2.89	13.0
	20.49 ± 1.80	9.3 ± 1.4	303.08 ± 5.29	12.5

C = compression force; CS = crushing strength; W = weight; D = disintegration time.

RESULTS AND DISCUSSION

The granulation process is controlled reliably by the installed sensors. A complete survey of temperature, humidity, and airflow courses during heating of the powder, spraying granulating liquid, and drying is guaranteed (Fig. 3). Any interruptions during the process, such as clogging of the nozzles or overwetting of the fluidized bed, would be detected immediately due to the short response times of the sensors (Table 2).

Calibration of the sensors can be performed without greater efforts and leads to satisfying results concerning the precision (Table 1). The sensitivity of the sensors describes accurately variations of process parameters within narrow limits. As temperatures during the process vary between 20°C and 70°C, this range is covered completely by the calibrations. Relative humidities range from about 15% to 60% and consequently are well within the humidity levels during calibration (Table 1). Airflow rates during granulation are about 8 m/sec and are covered by the calibration of the anemometer.

Calibration of the peristaltic pump shows less sufficient data for the correlation coefficient (Table 3). The pump has deficiencies concerning the regularity of its speed. It is assumed that differences of granule properties can be reduced to the pump. Due to irregularities of the

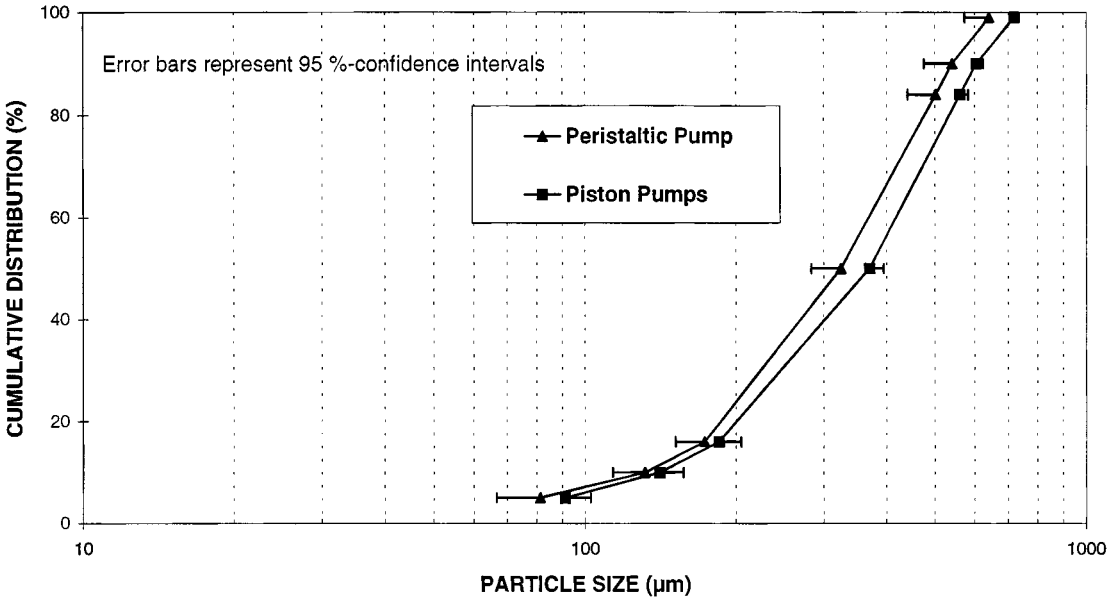

Figure 6. Comparison of the mean particle size distributions of granulations prepared with a peristaltic pump and two piston pumps, respectively.

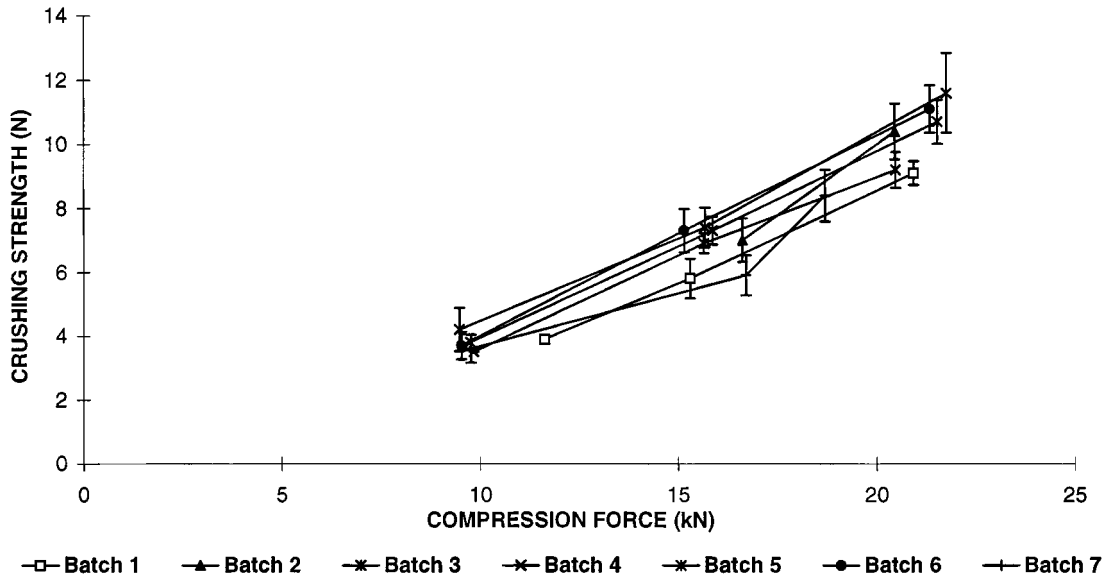

Figure 7. Crushing strengths of seven batches of lactose-PVP tablets granulated with the peristaltic pump as a function of the compression force ($N = 10$).

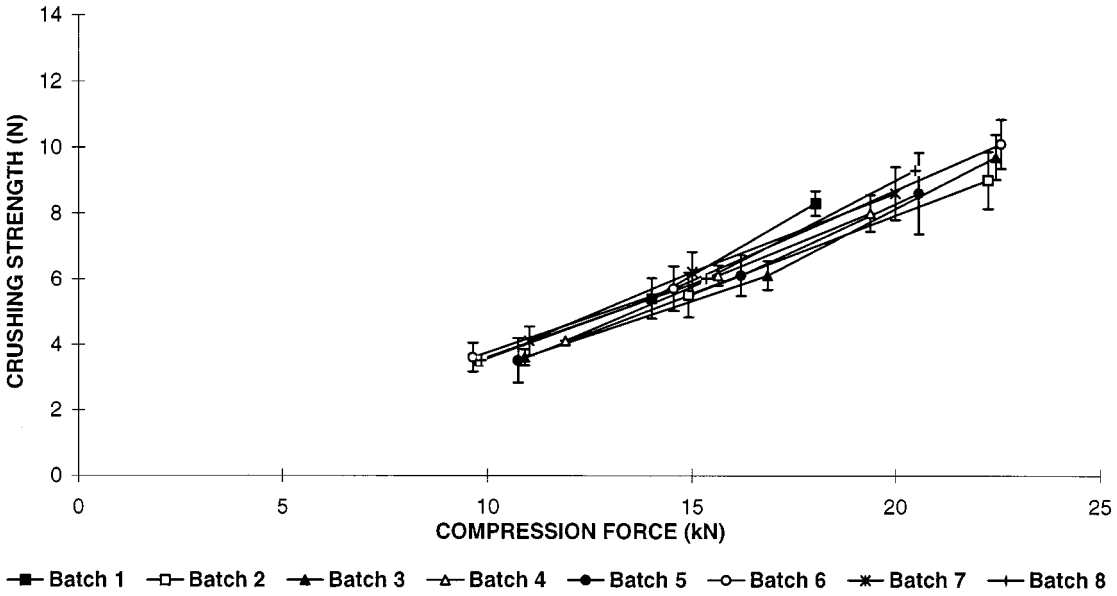

Figure 8. Crushing strengths of eight batches of lactose-PVP tablets granulated with piston pumps as a function of the compression force ($N = 10$).

pump speed, it is concluded that single bigger drops are developed at the nozzles that are sprayed into the powder bed. In several spots, overwetting takes place, and enlarged single granules are formed because of increasing humidity. The mean diameter of the granules can be explained by this assumption. The mean particle size d_{50} ranges from 269 μm to 420 μm, with an average of 325 μm (Fig. 4). Only 1 of 7 preparations has a significantly increased particle size of 420 μm, which can be explained by the influence of the peristaltic pump.

Considering the particle size distribution of the granules prepared using the piston pumps, the mean particle

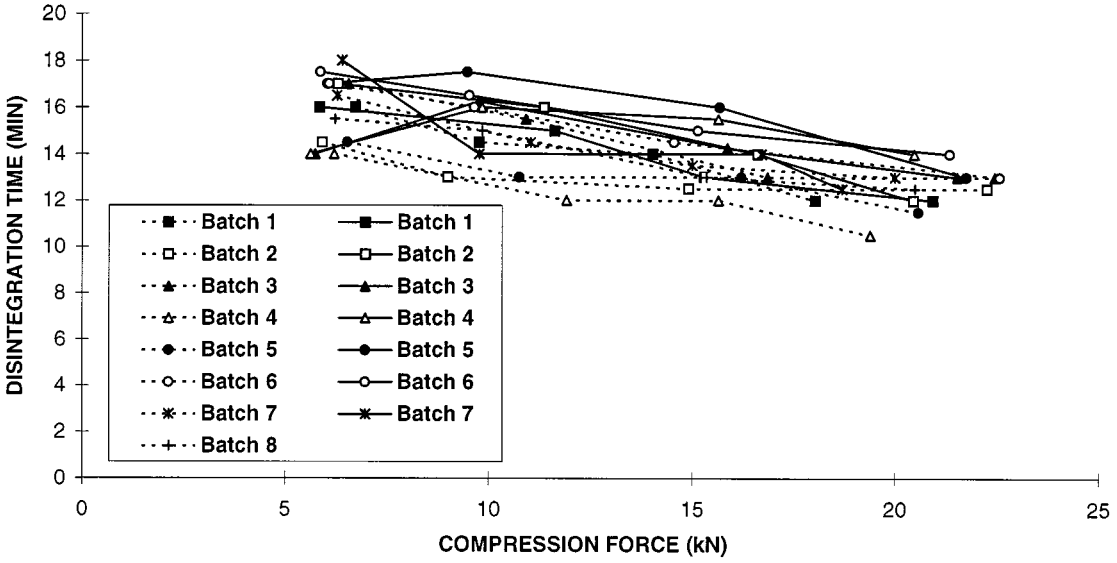

Figure 9. Disintegration times of 15 tablets of lactose-PVP tablets as a function of the compression force. Interrupted lines: piston pumps; continuous lines: peristaltic pump.

size d_{50} ranges from 305 μm to 414 μm, with an average of 370 μm (Fig. 5). Compared to the granules above, these granules are more homogeneous, as the error bars show. As no granulating liquid is ''wasted'' for single big agglomerates, for particle size enlargement, the slight increase in the mean particle size can be explained (Fig. 6). The particle size distributions of granules prepared with the piston pumps are shifted to higher particle sizes.

The construction of the Turbojet device leads to a powerful tangential movement of the powder bed in the product chamber, as well as to effective mixing in the vertical direction (Fig. 2). The granules are in constant movement, and good heat transition is guaranteed. Due to the location of the nozzles at the bottom of the fluidizing chamber, the complete amount of granulating liquid is sprayed into the powder bed. Spray-drying of the granulating liquid before reaching the particles does not occur, and the liquid is used completely for agglomeration of the powder. Correct adjustment of the pressures for atomizing air and microclimate prevent wetting of the walls of the product chamber. Any growth of encrustations on the walls of the product chamber is avoided. The construction of the nozzles with additional microclimate shows the advantage that clogging of the nozzles did not occur even once during the several processes.

Temperature of the fluidizing air is kept constant at 50°C ± 1°C during the whole process by the heater control. Inlet airflow can be controlled easily by the attached anemometer and adjusted with a potentiometer, varying the power of the ventilator which provides the airflow. With correct adjustment, the bed height expansion is about two times the diameter of the product chamber.

Because the cleaning of the dynamic filters happens continuously, the granulation process is not affected and no interruptions of the spraying are necessary. The humid exhaust air leaves the apparatus without being held back by the filters. An overwetting of the powder bed does not occur.

Granules obtained show the typical attributes of products derived from fluid-bed granulators. They have high porosities and an irregular rough surface. The poured and tapped densities and the Hausner value show no relevant differences between the batches (Table 4). Differences in the mean particle size could be explained by slight instabilities in the flow rate of the peristaltic pump. Particle size distributions show the same course (Figs. 4 and 5).

Tablet properties are controlled by the amount of binder. As this amount was constant for all preparations, the crushing strengths of the tablets as a function of the compression force show the same course (Figs. 7 and 8). An increase of the compression force leads to increased crushing strength of the tablets. As the hardness tester is only able to measure hardnesses up to 3 N, the very soft tablets produced at compression forces of 5 kN could not be tested. The collectively low crushing strengths are found to derive both from the process and from the formulation, which contains only 2.5% binder. Products from fluidized bed granulations show less granule hardness and greater plastic deformability compared with products made by agitation granulation (15).

Figure 9 shows the disintegration times as a function of the compression force. Increasing compression forces lead to slightly shorter disintegration times. All 15 batches show the same course. No differences between the granules derived from either the peristaltic pump or the piston pumps can be detected. The decrease of disintegration times with increasing compression forces can be explained by decreasing porosities within the tablet. The influence of the disintegrant intensifies because the remaining space becomes smaller. With less space between particles inside the tablet, the disintegrant shows increasing efficiency, which results in shorter disintegration times.

CONCLUSIONS

The granulation process could be controlled reliably by the installed sensors. Data were transferred with sufficient frequency and speed to the data receiver to evaluate changes of the parameters. The sensors provided reliable data with sufficient precision.

The bottom spray technique in the tangential direction benefitted from using the total amount of granulating liquid for the formation of granules without any losses. Fluidizing with the Turbojet device led to fast heat convection from fluidizing air to particles and short drying times while the powder bed was in constant movement. The construction of the filter cleaning system offered the advantage of cleaning the filters and fluidizing the powder at the same time without any interruptions of the process.

Granules with good flow and tableting properties could be produced in this small-scale unit. Slight differences in particle size distributions derived from instabilities in the supply with granulating liquid due to irregularities of the peristaltic pump. This can be avoided by using a piston pump.

The increase of crushing strengths of the tablets with higher compression forces showed the typical behavior. Tablet properties of all 15 batches showed no significant

differences concerning crushing strength or disintegration times. As both parameters were mainly influenced by the amount of binder, which was constant for all 15 preparations, slight differences of the particle size distributions had no influence on tablet properties. No influence of the two types of pump used for delivering the granulating liquid on tablet properties could be detected.

REFERENCES

1. H. Rumpf, Grundlagen und Methoden des Granulierens, Chem. Ing. Tech., 30, 144–158 (1958).
2. A. Laicher, Th. Profitlich, and K. Schwitzer, Sprühgranulation und Trocknung von Granulaten in einer neuen Universalprozessanlage im Produktionsmaβstab, Pharm. Ind., 56, 276–281 (1994).
3. A. S. Rankell, M. W. Scott, H. A. Lieberman, F. S. Chow, and J. V. Battista, Continuous production of tablet granulations in a fluidized bed II. Operation and performance of equipment, J. Pharm. Sci., 53, 320–324 (1964).
4. T. Schæfer and O. Wørts, Control of fluidized bed granulation. I. Effect of spray angle, nozzle height and starting material on granule size and size distribution, Arch. Pharm. Chemi, Sci. Ed., 5, 51–60 (1977).
5. T. Schæfer and O. Wørts, Control of fluidized bed granulation. II. Estimation of droplet size of atomized binder solutions, Arch. Pharm. Chemi, Sci. Ed., 5, 178–193 (1977).
6. W. L. Davies and W. T. Gloor, Jr., Batch production of pharmaceutical granulations in a fluidized bed I: effect of process variables on physical properties on final granulations, J. Pharm. Sci., 60, 1869–1874 (1971).
7. L. Juslin and J. Yliruusi, Granule growth kinetics and attrition of granules made of different materials in a fluidized bed granulator, Sci. Tech. Prat. Pharm., 6, 321–327 (1996).
8. H. Kokubo and H. Sunada, Effect of process variables on the properties and binder distribution of granules prepared in a fluidized bed, Chem. Pharm. Bull., 45, 1069–1072 (1997).
9. A. Menon, N. Dhodi, W. Mandella, and S. Chakrabarti, Identifying fluid-bed parameters affecting product variability, Int. J. Pharm., 140, 207–218 (1996).
10. T. Schæfer and O. Wørts, Control of fluidized bed granulation. V. Factors affecting granule growth, Arch. Pharm. Chemi, Sci. Ed., 6, 69–82 (1978).
11. P. Frake, D. Greenhalgh, S. M. Grierson, J. M. Hempenstall, and D. R. Rudd, Process control and end-point determination of a fluid bed granulation by application of near infra-red spectroscopy, Int. J. Pharm., 151, 75–80 (1997).
12. M. W. Scott, H. A. Lieberman, A. S. Rankell, and J. V. Battista, Continuous production of tablet granulations in a fluidized bed I. Theory and design considerations, J. Pharm. Sci., 53, 314–320 (1964).
13. H. Kristensen and T. Schæfer, Granulation. A review on pharmaceutical wet-granulation, Drug Dev. Ind. Pharm., 13, 803–872 (1987).
14. M. Banks and M. E. Aulton, Fluidised-bed granulation: a chronology, Drug Dev. Ind. Pharm., 17, 1437–1463 (1991).
15. H. Sunada, M. Hasegawa, T. Makino, H. Sakamoto, K. Fujita, T. Tanino, H. Kokubo, and T. Kawaguchi, Study of standard tablet formulation based on fluidized-bed granulation, Drug Dev. Ind. Pharm., 24, 225–233 (1998).